The effect of adding Copper on the structural and Creep Characteristics of Zn-0.5wt.%Al alloy

M. S. Sakr, M. M. Mostafa, H. S. Mohamed and N. M. Mahmoud

Abstract— The creep tests for the $\mathrm{Zn}-0.5\mathrm{wt.\%\,Al}$ and $\mathrm{Zn}-0.5\mathrm{wt.\%Al}-0.3\mathrm{wt.\%\,Cu}$ alloys were carried out at different applied stresses ranging from 15.6 MPa to 23.4 MPa and temperatures ranging from 433K to 553K. The values of the transient creep parameters β and n and the steady state creep parameters m and $\dot{\epsilon}_{st}$ exhibited two peak values at $473K$ and $523K$ for the two test alloys. The activation energies of the steady state creep were found to be *43.7 KJ/mole, 90.6 KJ/mole, 94.9 KJ/mole for the first alloy, and , 39.3KJ/mole, 52.8 KJ/mole*, *71.2 KJ/mole for the second alloy* in the low, intermediate and high temperature regions respectively. The microstructures of the two alloys have been investigated using the X-ray diffraction analysis (XRD) and the optical microscope.

Index Terms— Zn-rich-Al alloys, Creep test, XRD, Optical microscope, Phase transformation, Activation energies.

1 Introduction

In recent years Zn-rich-Al alloys with the addition of iron or copper used in a wide range for engineering. The addition of alloying elements reinforce, the corrosion resistance, elastic modulus, and yield strength under different stresses and temperatures without having a major prejudicial effect on superplastic behavior [1]. Zn-Al alloys are widely used as bearing materials unguarded at high loadings that operate in mining; milling machines, rope hoisting units and used also in automotive application [2, 3].

The copper addition to Zn-Al alloy could improve the mechanical properties, melting range, microstructure and spread ability [4-6].

Y. H. Zhu [7] studied the microstructural changes and phase transformation of Zn-Al alloy with Cu additives, which explained by the Gibbs free energy. Zn-Al-Cu alloy was also tested by R. Michalik et al. [8] showed a major effect of aging on the structure, hardness and wear resistance. Zn-Al-Cu alloys characterized with improving the strength and increase hardness because of precipitation of Cu and Al in Zn [9].

A little attention information available on the effect of phase transformation on the variation of the microstructure and the creep characteristics.

The present work aims studying the influence of copper additive on the properties of microstructure and creep charac teristics of $Zn-0.5wt.\%\,Al$ during phase transformation.

2 Experimental procedure

$Zn-0.5wt.\%\,Al$ and $Zn-0.5wt.\%\,Al-0.3wt.\%\,Cu$ alloys were prepared by Zn, Al, and Cu with purity 99.9% by a melting method under vacuum in a high purity graphite crucible.

The ingots were cast and cold drawn to 0.8 mm in diameter wire for creep measurements and 0.3 mm thickness sheets for microstructure examination. The wires and sheet were homogenized at $573K$ for $24h$ and cools slowly till room temperature within a cooling rate of $11\times10^{-3}\ KS^{-1}$. This heat treatment allowed the three phases to exist [10]. The chemical composition for the tested alloys was verified by analyzing the energy dispersed X-ray analysis.

Creep measurements for test samples have been investigated by using a conventional testing machine mentioned elsewhere [11] through a strain resolution equal to 10^{-5} and constant stresses ranging from $15.6MPa$ to $23.4MPa$ in the temperature range from $433K$ to $553K$ in steps of $10K$.

The treated sheet specimen was etched using the solution of $90ml$ alcohol and $10ml$ nitric acid. The microstructure examination was carried out using Nikon optical microscope, Philips X-ray diffractometer ($PW3710$) through copper K_α radiation of wavelength $1.54A^0$ and nickel filter.

3 Experimental Results and discussion

Isothermal creep curves of $(a)\ Zn-0.5wt.\%\,Al$ and $(b)\ Zn-0.5wt.\%\,Al-0.3wt.\%\,Cu$ alloys studied using various applied stresses ranging from $15.6MPa$ till $23.4MPa$ within various working temperatures ranging from $433K$ till $553K$ in steps of $10K$ ($Fig.1a,b$).

The temperature series for the creep curves is irregular at a temperature range from $463K$ to 493K and from 513k to 533K for the two alloys.

4 The transient creep

This type of creep could be presented by the equation [12].

$$\epsilon_{tr}=\beta t^{n} \qquad (1)$$

where: β and n are the transient creep parameters and t is the creep time in seconds.

- *N. M. Mahmoud is currently pursuing masters degree program in solid state in Ain shams university, Egypt, PH-+201113335955. E-mail: nohamohamed7@edu.asu.edu.eg*
  M. S. Sakr and M. M. Mostafa are currently professors of solid state in Ain shams university, Egypt, E-mail: mhussien47@hotmail.com
- *H. S. Mohamed is currently a doctor of solid state in Ain shams university, Egypt, E-mail: drhanansayed84@gmail.com*

The parameter β could be calculated from:

$$\ln \beta = \ln t_2 \ln \epsilon_{tr_1} - \ln t_1 \ln \epsilon_{tr_2} / \ln t_2 - \ln t_1 \qquad (2)$$

The parameter β was found to depend on the strain rate of the steady state creep ($\dot{\epsilon}_{st}$) through the relation:

$$\beta = \beta_0 (\dot{\epsilon}_{st})^{\gamma} \qquad (3)$$

where β_0 and γ are constants depending on the experimental conditions.

The relationship between $\ln \epsilon_{tr}$ and ln t is shown in ($Fig. 2a, b$). Abnormal creep was observed at $473K$ and $523K$ for both test alloys. Using the relation (2) the transient creep parameter β was calculated while the parameter n was calculated from the slopes of these lines. ($Fig. 3$) clarifies the temperature dependence of β and n for the test alloys. The parameters β and n exhibited peak values at $473K$ and $523K$ for both test alloys.

A marked dependence about the transient creep parameter β on steady state strain rate ($\dot{\epsilon}_{st}$) verifying the relation(3), ($see\ Fig. 4$).

The activation energy for the transient creep of the two alloys were calculated within the slopes of the straight lines related to $ln\beta$ and $(1000/T)$($Fig. 5$). The present results gave activation energies of 25.8, 27.6 and 35.5KJ/mole for the first alloy and 17.5,22.5 and 23.7KJ/mole for the second alloy at the low, intermediate and high-temperature deformation regions, respectively. These values refer to the dislocation mechanism in the low and intermediate deformation regions and to viscous glide in the high temperature deformation region [13].

5 The steady State Creep

The steady state creep was commonly considered as due to some sort of balance between strain hardening and recovery. The applied stress for creep deformation is marked by depending on the strain rate according to the relation [14]:

$$\sigma = k\ (\dot{\epsilon}_{st})^m \qquad (4)$$

where σ is the applied stress and ($\dot{\epsilon}_{st}$) is the steady state creep rate and k is constant for the given testing conditions.

At the low temperature region, it was found that the parameters $\dot{\epsilon}_{st}$ and m for both test alloys have been increased with increasing the deformation temperture (see Fig. 6a, b and Fig. 7a, b). These observations might be due to the coarsening of the α-phase and β-phase. These processes comprise dissolution at some places and precipitations at other ones. These processes enhance the recovery processes and increase the density of mobile dislocations.

Meanwhile, these parameters $\dot{\epsilon}_{st}$ and m have increased also with temperature in the intermediate deformation temperature. This observation could be because of the dissolution of α-phase in β-phase which completed at $523K$ [15].

Besides, the parameters $\dot{\epsilon}_{st}$ and m for both alloys have been increased again with temperature in the high temperature deformation regions. These observations might be because of completing the dissolution of α-phase in β-phase and homogenization.

The activation energies of the steady state creep for both alloys found to be 43.7, 90.5 and 94 KJmole for the first alloy and 39, 52.8 and 71.2KJ/mole for the second alloy (Fig. 8). These values show the dislocation mechanism and grain boundary sliding at low and intermediate temperature deformation regions and self- diffusion of zinc in the high temperature deformation regions [15].

6 THE ROLE OF Cu ADDITION TO THE $Zn - 0.5wt.\%\ Al - 0.3wt.\%\ Cu$ ALLOY ON THE CREEP CHARACTERISTICS

In the liquid state the three elements of the alloy $Zn - 0.5wt.\%\ Al - 0.3wt.\%\ Cu$ are completely mutually soluble. On cooling η-phase (Zn-rich phase of hcp structure with substitutional copper atoms) precipitates first at $696K$ [16]. The η-phase would be surround by the molten β-phase (Zn-rich phase of hcp structure with substitutional Al atoms).The complete solidification of the β-phase would occur at419^0c [17]. By further cooling some Al- atoms would be precipitated from the β-phase at $523K$ [17], to make the β-phase goes to the actual proportion percentage at this temperature.Therefore, the η- phase would be uniformly distributed among the other solid phases. This behavior has increased the interfaces boundaries between the different phases. This behavior enhanced the migration of the point defects in the matrix to these natural sinks. Therefore, the η-phase particles have an important effect for grain refining. These explain the reasons of the higher values of the creep parameter $\beta, n, \dot{\epsilon}_{st}$ and m of the ternary alloy in comparison with those of the binary alloy.

7 The Microstructure Analysis

The specimens were heated at 503k for 2h and then cooled until room temperature at cooling rate about ($11 \times 10^{-3}\ KS^{-1}$) to remove the lattice defects which produced during the drowning process. The optical micrographs of both alloys are shown in (Fig. 9).

Fig. (10) shows the X-ray diffraction patterns where the phases of the binary are shown as follows:

$$\alpha\ (111), \beta\ (101), \beta\ (102), \beta\ (103), \beta\ (110)$$
$$Al\ (111), Zn\ (101), Zn\ (102), Zn\ (103), Zn\ (110).$$

And the phases of ternary are shown as follows:

$$A\ (111), \beta\ (101), \eta\ (200), \beta\ (102), \beta\ (103), \beta\ (110)$$
$$Al\ (111), Zn\ (101), Cu\ (200), Zn\ (102), Zn\ (103), Zn\ (110).$$

The crystallite size η, calculated from Scherrer's formula:

$$D = 0.94\ \lambda / \eta \cos\theta \qquad (5)$$

where λ is the X-ray wavelength, θ is the Bragg's angle and η is the full-width at half maximum of the Bragg peak. The Lattice strain (ϵ) is calculated by the relation of $\eta \cos\theta\ /\lambda$ versus $\sin\theta\ /\lambda$ plot using the relation [18]:

$$\eta \cos\theta/\lambda = 1/D + 2\epsilon \sin\theta/\lambda \qquad (6)$$

The dislocation density δis given by:

$$\delta = 1/D^2 \qquad (7)$$

The temperature dependence of the parametersϵ, η and δ are shown in (Fig. 11).

The values of the parameters ϵ and δ of the ternary alloy are less than those of the binary alloy.

Thus, this observation illustrates that the addition of copper to the third alloy has an important effect grain refining.

Therefore, the microstructure investigations confirm the above-mentioned mechanisms.

8 CONCLUSIONS

1- The creep parameters β , n of the transient creep and m and $\dot{\epsilon}_{st}$ of the steady state creep have exhibited peak values at $473K$ and $523K$.

2- The creep parameters of the $Zn-0.5wt.\%Al-0.3wt.\%Cu$ were found to be higher than those of the $Zn-0.5wt.\%Al$ alloy.

3- The activation energies of the steady state creep were found to be *(43.7 KJ/mole, 90.6 KJ/mole, 94.9 KJ/mole),and (39.3KJ/mole, 52.8 KJ/mole* and *71.2 KJ/mole)* in the low, intermediate and high temperature regions for the two alloys, respectively. These values suggest grain boundary sliding or migration mechanism and volume diffusion mechanism of Zn, respectively.

4- The X-ray diffraction studies have been carried out. The values for the internal strain, the dislocation density σ and the crystallite size D of the two alloys were calculated.

5- The values of ϵ and δ for the ternary alloy were found to be lower than those of the binary alloy. On the other hand, the values of the crystallite size η for the ternary alloy were found to be higher than those of the binary alloy.

6- Therefore, the addition of Cu to $Zn-0.5wt.\%Al-0.3wt.\%Cu$ has an important effect of grain refining process.

REFERENCES

[1] J. D. Velleqo, Material Research, (2014) 1715.
[2] M. Babic, R. N. Vic, Tribology in industry, 26, (2004) 1.
[3] S. Murphy, T. Savaskan, Wear, 98, (1984) 151.
[4] S. J. Kim, K. S. Kim, S. S. Kim, C.Y. Kang and K. Suganuma, Materials Transaction, 49, (7), (2008) 1531.
[5] T. Savaskan, G. Purcek, A. P. Hekimoglu, Tribology Letters 15, (2003)) 257.
[6] B. K. Prasad, Wear 240, (2000) 100.
[7] Y. H. Zhu, Materials Transaction,45, (11), (2004) 3083.
[8] R. Michalik, A. Tomaszewska, Arch. Metall. Mater., 61, (1), (2016) 289.
[9] R. Michalik, Arch. Metall. Mater., 58, (1), (2013).
[10] L. E. Larson, Acta. Met.15, (1967) 35.
[11] A. F. Abdel-Rehim, M. S. Sakr, M. M. El-Sayed, M. A. Abdel-Hafez, Journal of Alloys and Compounds 607, (2014) 157.
[12] J. Friedel, Pergamon press, London,304, (1964) 317.
[13] M. S. Sakr, A. E. E. Abel-Reheim, A. A. El-Daly, Egypt. J. sol,7, (1), (1985) 42.
[14] W. A. Backofen, I. R. Turner and D. H. Avery, Trans. A. S. M, 57, (1964) 980.
[15] M. S. Sakr, A. E. E. Abdel-Reheim, A. A. EL-Daly, phys. Stats. Sol. 94, (1986) 561.
[16] M. Hansen, K. Anderko, "Constitution of Binary Alloys", Mc graw-Hill, 630 (1958).
[17] M. Hansen, K. Anderko, "Constitution" of binary alloys, Me-Graw-Hill, New York, 149 (1958).
[18] B. E. Warren, Rep. Prog., Metals, 8, (1959) 147.

FIGURE CAPTIONS

Fig. (**1**) Creep curves at an applied stress 15.6MPa and different working temperatures for $(a)Zn-0.5wt.\%Al$ and $(b)Zn-0.5wt.\%AL-0.3wt.\%Cu$,where:
(1)433, (2)443, (3)453k, (4)463, (5)483k, (6)473k, (7)493k, (8)503k, (9)513k, (10)533k, (11)523k, (12)543k, (13)553k.

Fig. (**2**) The Relation between $\ln \epsilon_{tr}$ and $\ln t$ for (a) $Zn-0.5wt.\%Al$ and (b)$Zn-0.5wt.\%Al-0.3wt.\%Cu$ alloys at different working temperatures and different stresses.

Fig. (**3**) The temperature dependence of the Creep parameters β and n on the working temperature at different applied stresses for (a) $Zn-0.5wt.\%Al$ and (b)$Zn-0.5wt.\%Al-0.3wt.\%Cu$ alloys.

Fig. (**4**) The linear relation between $\ln \beta$ and $\ln \dot{\epsilon}_{st}$ at different applied stresses in the three temperature deformation region for: (a)$Zn-0.5wt.\%Al$ and (b)$Zn-0.5wt.\%Al-0.3wt.\%Cu$ alloys.

Fig. (**5**) The relation between $\ln \beta$ and $1000/T$ at different stresses for: $(a)Zn-0.5wt.\%Al$ and $(b)Zn-0.5wt\%Al-0.3wt.\%Cu$ alloys.

Fig. (**6**) The relation between $\ln \sigma$ and $\ln \dot{\epsilon}_{st}$at different working temperatures for $(a)Zn-0.5wt.\%Al$ and $(b)\ Zn-0.5wt.\%Al-0.3wt.\%Cu$ alloys.

Fig. (**7**) The temperature dependence of the parameters $\dot{\epsilon}_{st}$and m for: $(a)Zn-0.5wt.\%Al$ and $(b)Zn-0.5wt.\%Al-0.3wt\%Cu$ alloys.

Fig. (**8**) The relation between $\ln \dot{\epsilon}_{st}$and $1000/T$ for: $(a)Zn-0.5wt.\%Al$ and $(b)Zn-0.5wt.\%Al-0.3wt.\%Cu$ alloys.

Fig. (**9**)(a) and (b) shows the optical microscope for the binary and ternary alloys respectively.

Fig. (**10**. **1**, **2**) Shows the XRD results for the binary and ternary alloys respectively.

Fig. (**11**) Shows the temperature dependence of the parameters ϵ, D, δ for both alloys where: (A), (B) represents binary and ternary alloys respectively.

FIGURES

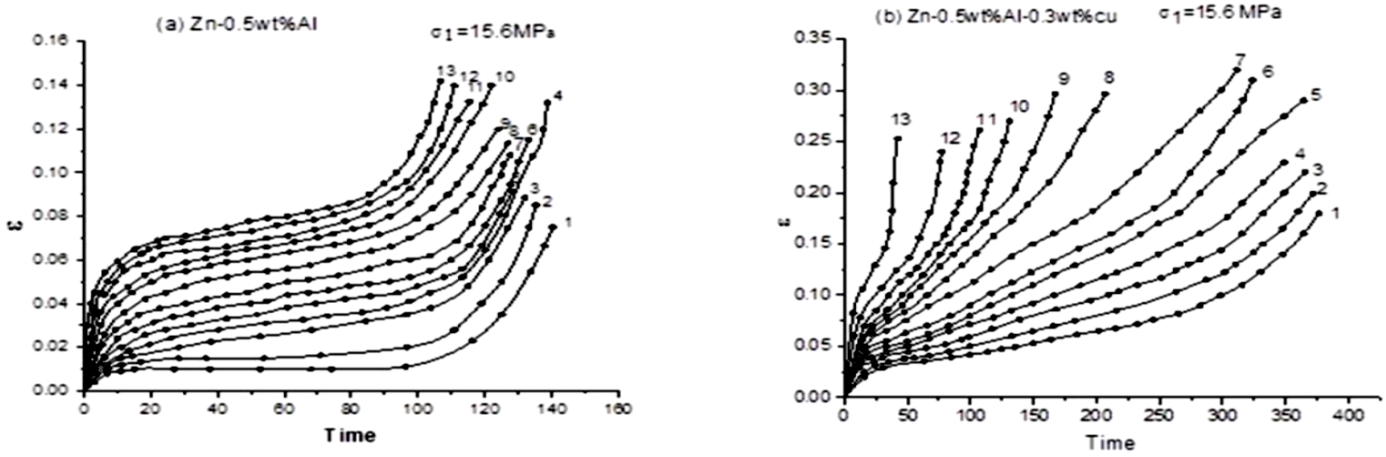

Fig. 1. Creep curves at an applied stress $15.6MPa$ and different working temperatures for $(a)Zn-0.5wt.\%Al$ and $(b)Zn-0.5wt.\%AL-0.3wt.\%Cu$, where: (1)433, (2)443, (3)453k, (4)463, (5)483k, (6)473k, (7)493k, (8)503k, (9)513k, (10)533k, (11)523k, (12)543k, (13)553k.

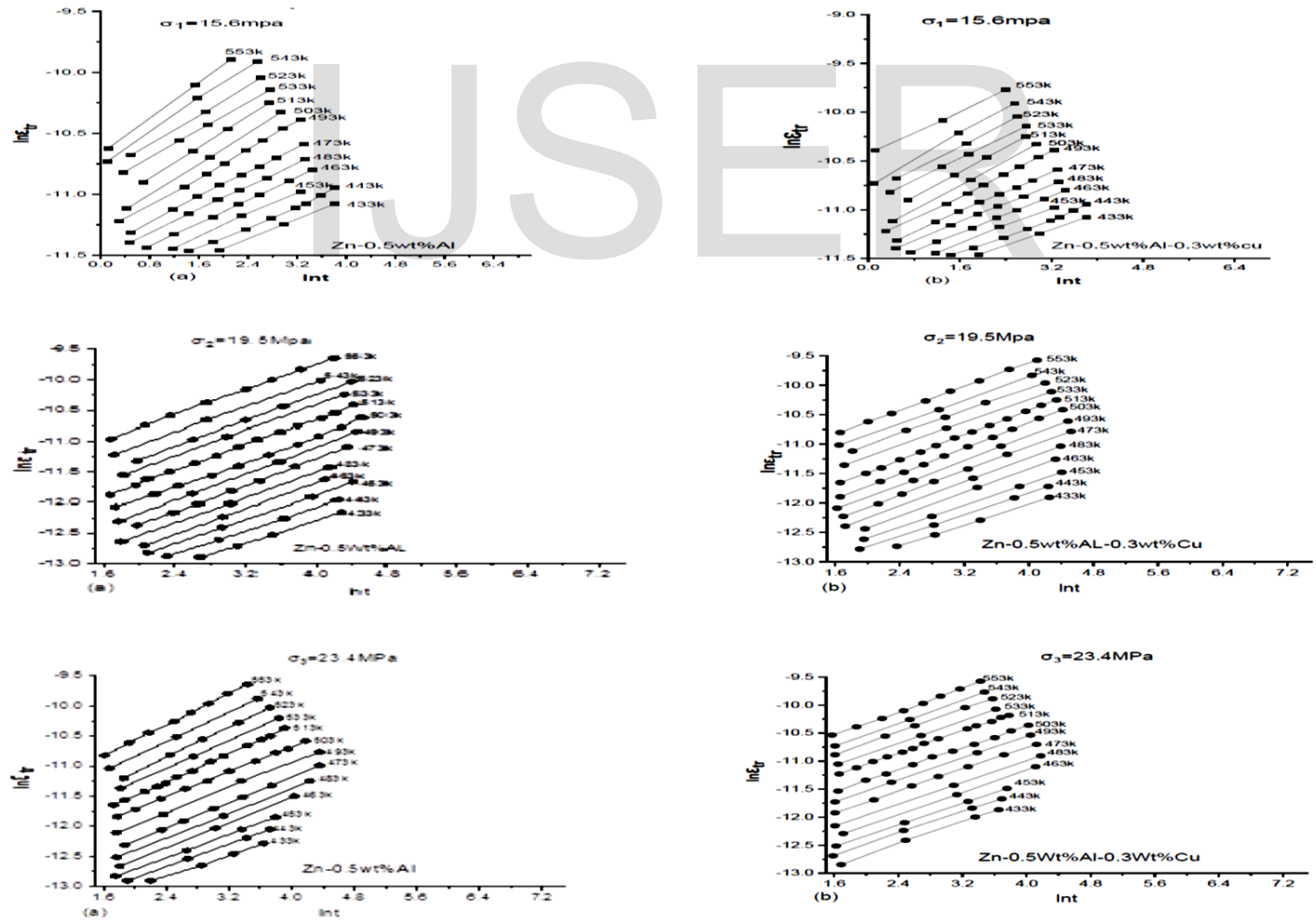

Fig. 2. The Relation between $ln\ \epsilon_{tr}$ and ln t for (a) $Zn-0.5wt.\%Al$ and (b) $Zn-0.5wt.\%Al-0.3wt.\%Cu$ alloy at different working temperatures and different stresses.

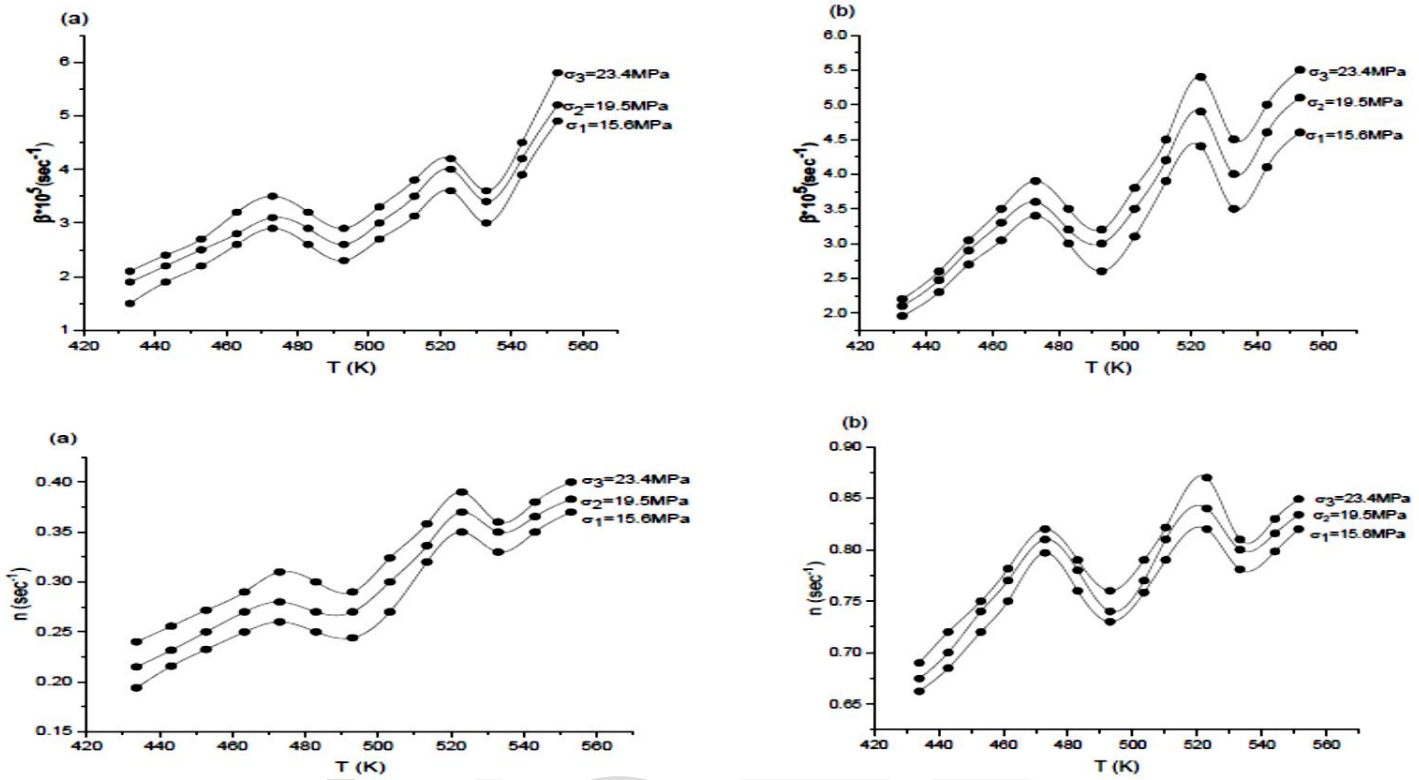

Fig. 3. The temperature dependence of the Creep parameters β and n on the working temperature at different applied stresses for $(a)\ Zn-0.5wt.\%Al$ and $(b)Zn-0.5wt.\%Al-0.3wt.\%Cu$ alloys.

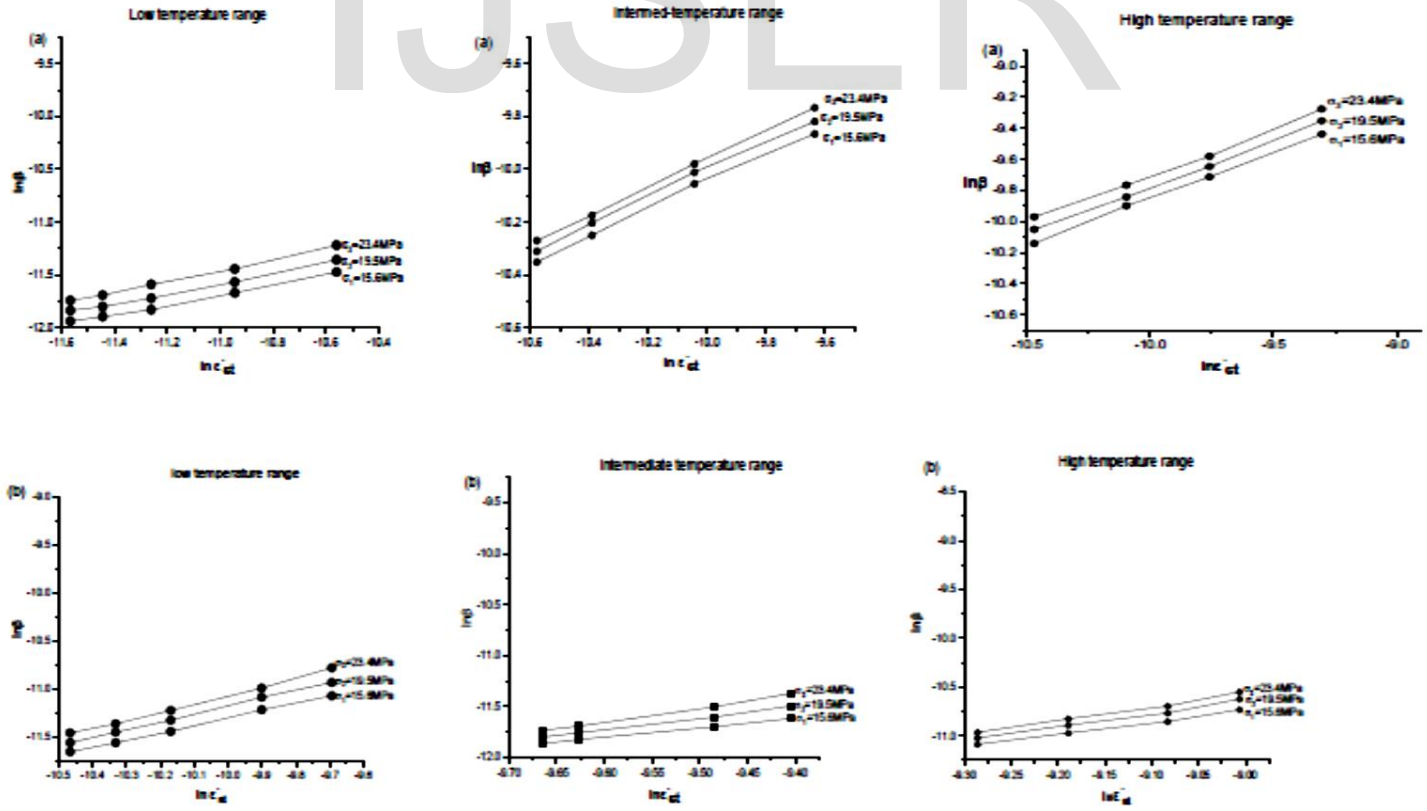

Fig. 4. The linear relation between $\ln\beta$ and $\ln\dot{\epsilon}_{st}$ at different applied stresses in the three temperature deformation region for: (a)$Zn-0.5$wt. %Al and (b)$Zn-0.5$wt. %$Al-0.3$wt. %Cu alloys.

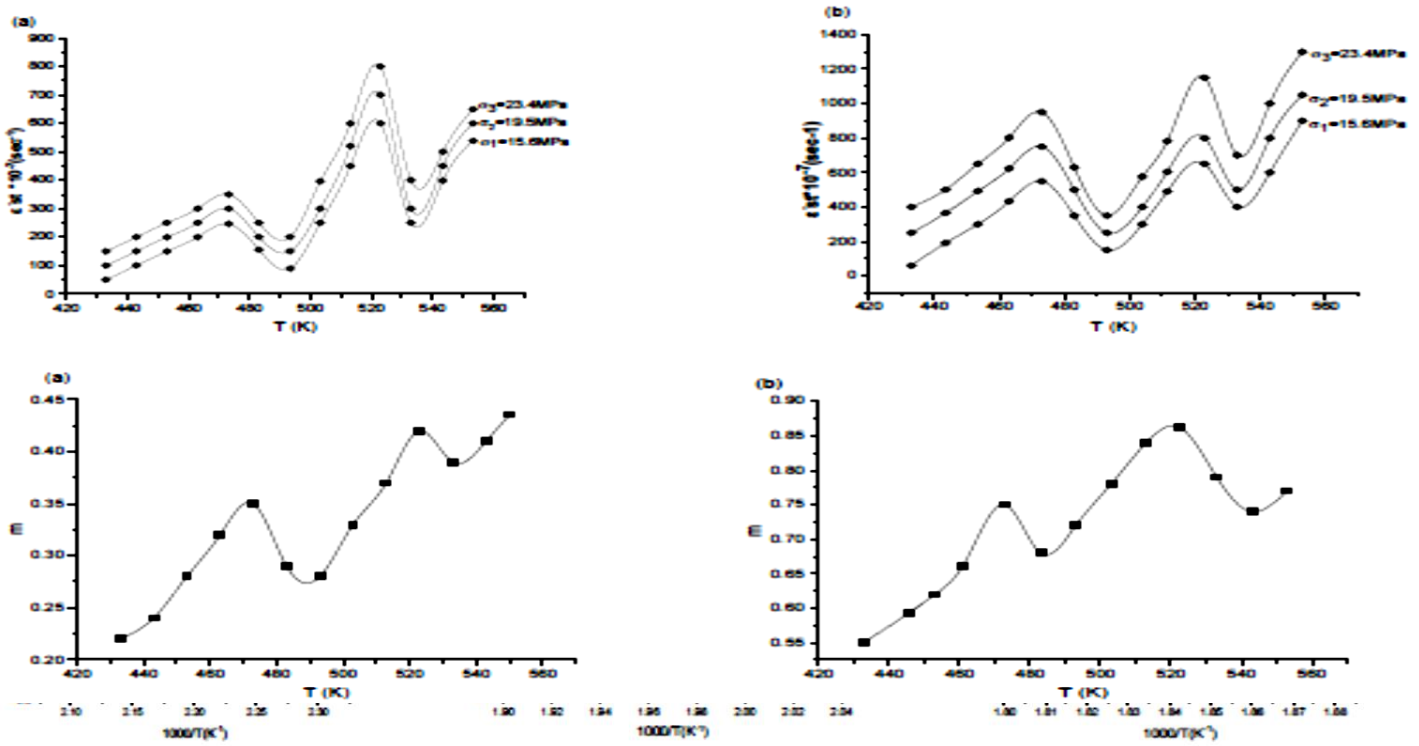

Fig. 5. The relation between $\ln\beta$ and $1000/T$ at different stresses for: $(a) Zn-0.5wt.\%Al$ and $(b)\ Zn-0.5wt\%Al-0.3wt.\%Cu$alloys.

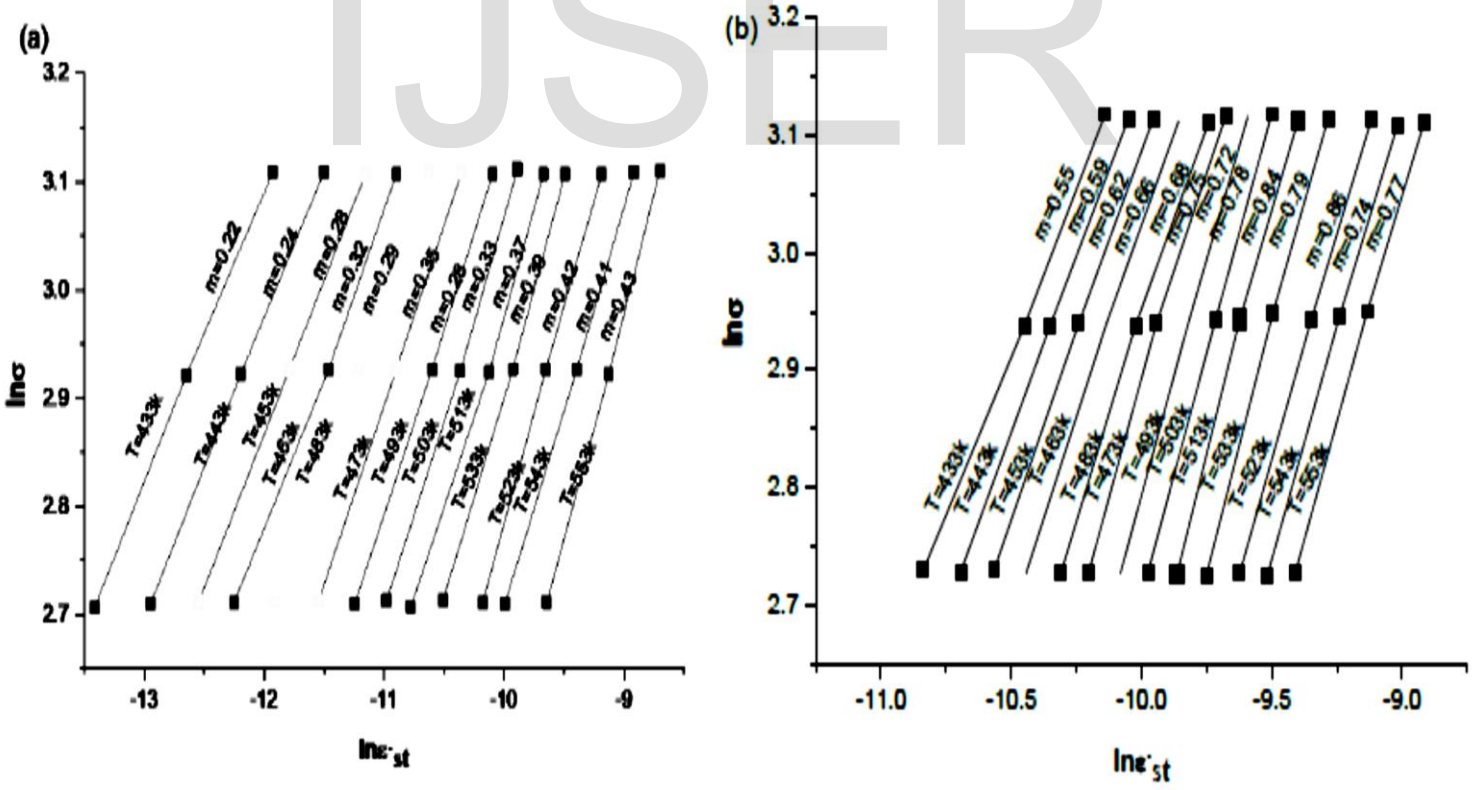

Fig. 6. The relation between $ln\ \sigma$ and $ln\ \dot{\epsilon}_{st}$at different working temperatures for $(a) Zn-0.5wt.\%Al$ and $(b)\ Zn-0.5wt.\%Al-0.3wt.\%Cu$ alloys.

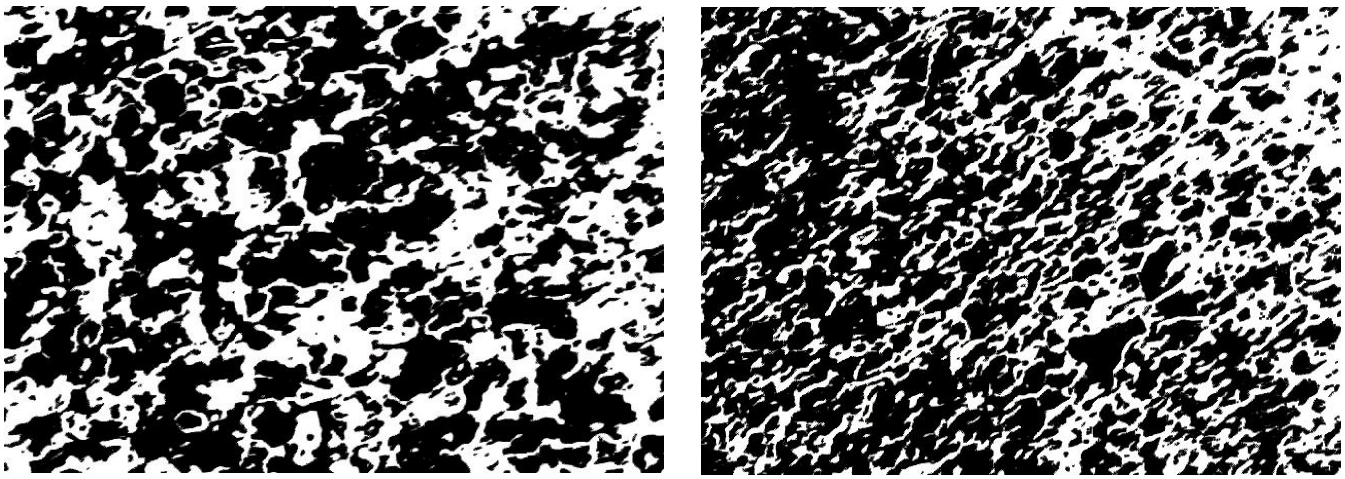

Fig. 7. The temperature dependence of the parameters $\dot{\epsilon}_{st}$and m for: $(a)Zn-0.5wt.\%Al$ and $(b)Zn-0.5wt.\%Al-0.3wt\%Cu$ alloys.

Fig. 8. The relation between $\ln \dot{\epsilon}_{st}$and $1000/T$ for: $(a)Zn-0.5wt.\%Al$ and $(b)Zn-0.5wt.\%Al-0.3wt.\%Cu$ alloys.

(a) (b)

Fig. 9. (**a**) and (b) shows the optical microscope for the binary and ternary alloys respectively.

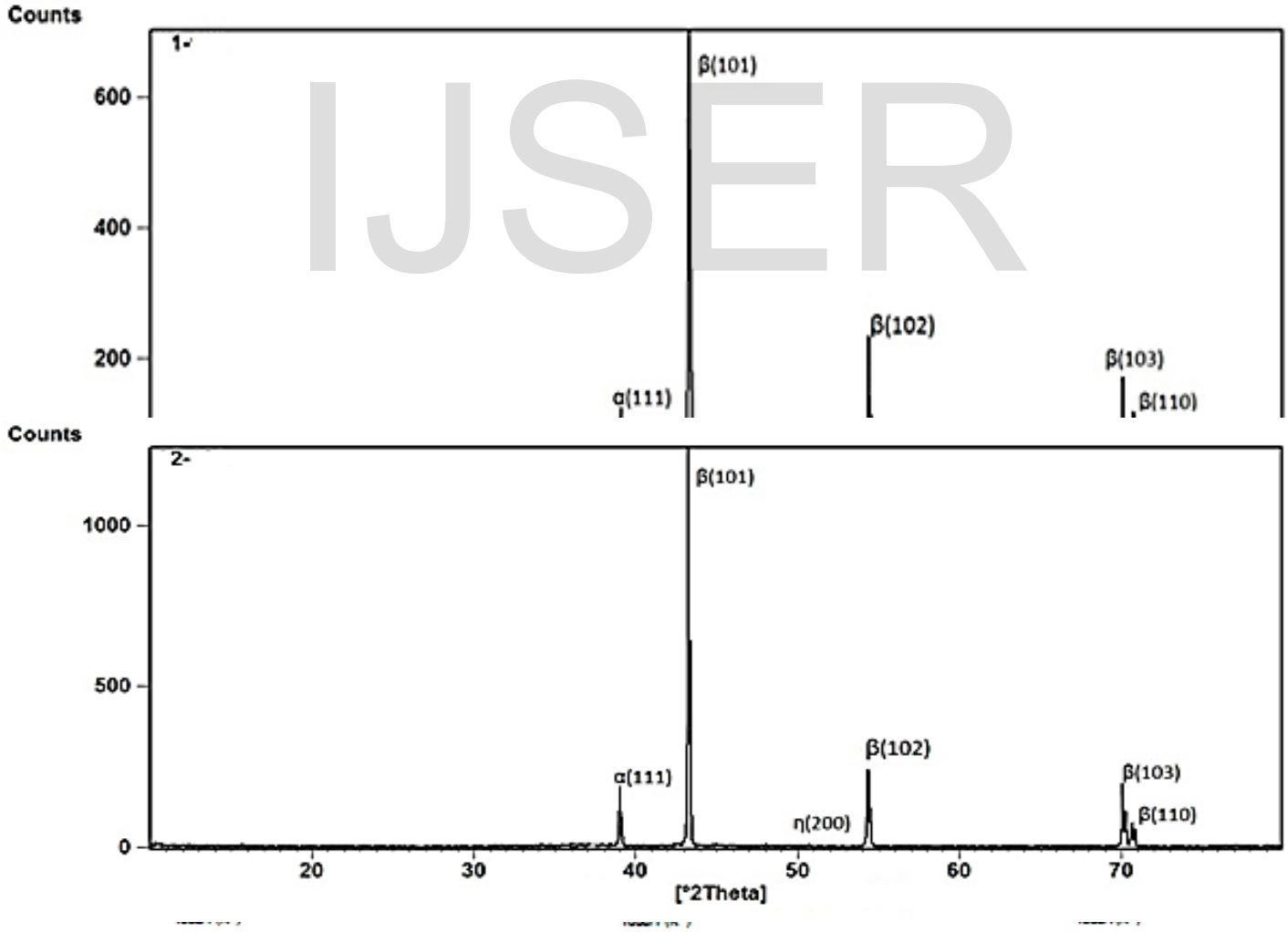

Fig. 10. (1, 2) shows the XRD results for the binary and ternary alloys respectively.

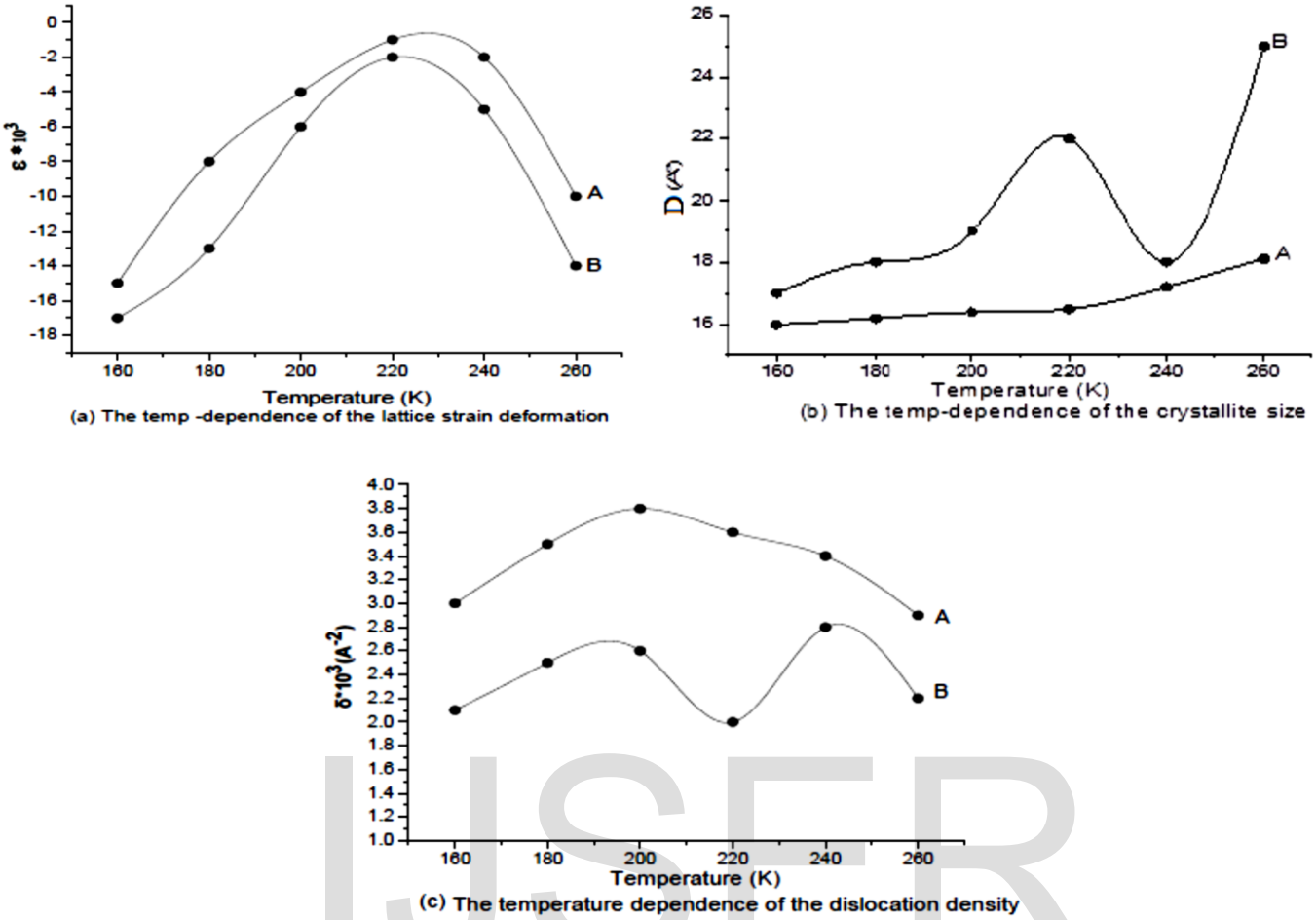

Fig. 11. shows the temperature dependence of the parameters ϵ, D, δ for both alloys where: $(A), (B)$ represents binary and ternary alloys respectively.